JMEPEG (2010) 19:395–400
DOI: 10.1007/s11665-009-9512-9

1059-9495/$19.00

Equicohesion: Intermediate Temperature Transition of the Grain Size Effect in the Nickel-Base Superalloy PM 3030

Michel Nganbe and Atef Fahim

(Submitted April 15, 2009)

The intermediate temperature transition of the grain size effect on the yield strength of PM 3030 is investigated using compression tests from room temperature to 1200 °C. It is found that grain boundary strengthening is strong at low temperature which is consistent with conventional Hall–Petch hardening. However, the grain boundary contribution to strength diminishes exponentially at intermediate temperature and vanishes at the equicohesion point. Above the equicohesion point, finer grain structure leads to material softening primarily due to grain boundary diffusion and deformation processes. Maximum softening occurs at $T_{soft\text{-}max}$ which is about 70% of the melting point, then decreases logarithmically with further increase in temperature, and vanishes at the melting point. This can well be rationalized by the overwhelming dominance of volume diffusion over grain boundary diffusion at temperatures close to the melting point, which decreases the impact of grain size on material strength. An exponential transition from the Hall–Petch behavior to the diffusion-based behavior provides an overall better fit of test data as compared to a linear transition. This study provides a contribution to the understanding of equicohesion and variation of the grain size effect on material strength and can be particularly crucial for components used at intermediate temperature.

Keywords equicohesion temperature, grain boundary diffusion, grain boundary softening, grain boundary strengthening, intermediate temperature transition

1. Introduction

The concept of grain boundary hardening has been proven very efficient for low temperature applications where finer grain structure of a material generally shows increased strength and toughness as compared to coarse grain and single crystal structures of the same material. This Hall–Petch strengthening phenomenon (Ref 1-3) has been the subject of extensive and continuing research and modeling in the past decades, and is today a solid element of fundamental mechanical engineering knowledge. In addition, the concept of single crystals has been proven most appropriate for extremely high temperature applications where polycrystalline fine grain structure of materials leads to softening, premature damage, and failure. This softening effect is primarily due to grain boundary diffusion and the ensuing damage processes (Ref 4, 5). To date, the behavior and the phenomenon governing the transition from grain boundary strengthening at low temperature to grain boundary weakening at high temperature have not been adequately investigated, and very little information can be found in the scientific literature. Therefore, decision making on whether finer or coarser grain provides the higher strength for a given intermediate temperature application is often confused and based on past experiences rather than on scientific or engineering knowledge. An in-depth study of this transition regime would enhance the understanding of prevalent deformation mechanisms at different temperatures, and how these mechanisms relate to grain boundaries, grain size and material's strength. Furthermore, the notion of equicohesion (Ref 6-8) is often overlooked nowadays when considering material strength at intermediate temperature. A better understanding of this notion and thereby of the variation in grain size effect on material strength can be very crucial for intermediate temperature applications as well as for material, process, design, and cost optimizations in industry.

Michel Nganbe and **Atef Fahim**, Department of Mechanical Engineering, University of Ottawa, 161 Louis-Pasteur, Ottawa, ON K1N 6N5, Canada. Contact e-mail: mnganbe@uottawa.ca.

2. Materials, Experimental Methods, and Observations

This study focuses on two isotropic batches of PM 3030 (R90 and R901315) manufactured by Plansee GmbH, Lechbruck, Germany, with a nominal chemical composition in weight percentage of 17Cr-2Mo-3.5W-2Ta-6.6Al-1.1Y_2O_3 with balance nickel. R90 and R901315 have isotropic grain sizes of 1 and 17 μm (see Fig. 1), respectively. All the batches are manufactured by mechanical alloying (Ref 9, 10) followed by hot isostatic pressing (HIP). An additional secondary recrystallized batch (R34, Ref 11) is used as a reference material. It has coarse and strongly elongated grains with a mean grain length of over 70,000 μm and an equivalent mean diameter of 600 μm. This results in a grain aspect ratio (GAR) of over 116, and would

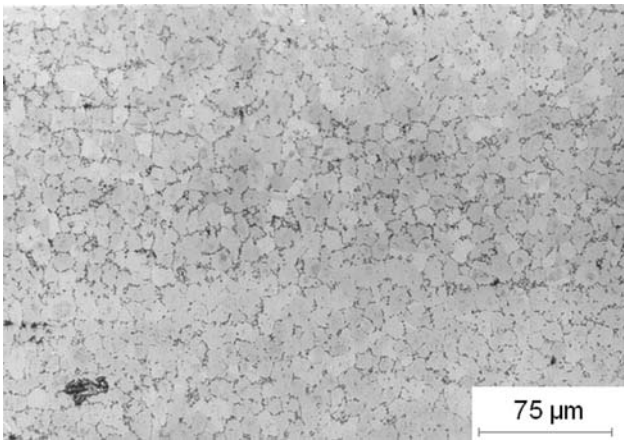

Fig. 1 Microstructure of the isotropic batch R901315 of PM 3030 with grain size = 17 µm. The microstructure of R90 is similar, however with a grain size of 1 µm

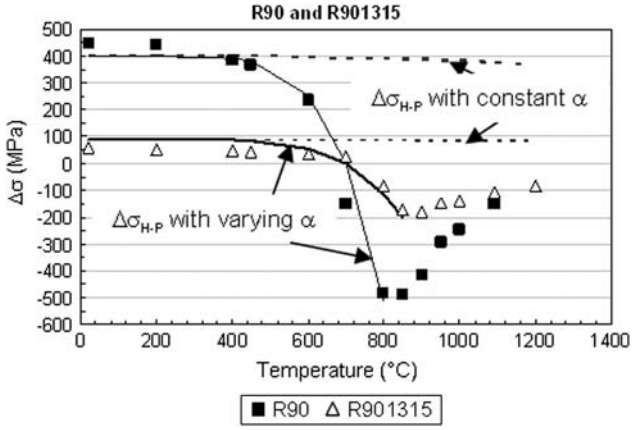

Fig. 2 Temperature-dependent variation of the grain boundary strengthening contribution in PM 3030 for both R90 and R901315: measurement data, curves resulting from the conventional Hall–Petch model with constant grain strengthening coefficient (hatched) and from the modified Hall–Petch model with temperature-dependent grain strengthening coefficient (solid) are plotted

allow it to be considered to have a quasi-static mechanical strength similar to that of a single crystal. This assumption is necessary here because PM 3030 cannot be manufactured in a single crystal structure due to limitations of the powder metallurgy manufacturing route, including strengthening of Y_2O_3 dispersoids that can prevent grain growth and the tendency of dispersoids to coarsen, dissolve, or segregate during heat treatments at extremely high temperatures.

It has been shown that coarse and elongated grain superalloys such as R34 that have been strengthened by oxide dispersion can be as strong as single crystal superalloys. This is due to the limit on grain boundary deformation and damage processes resulting from the very high GAR values (Ref 12, 13). In addition, the grain boundary strengthening contribution in R34 is practically zero due to the extremely large grains. R34 has a fiber texture; its grains show a ⟨101⟩ crystallographic orientation and are elongated in the axial direction, coincident with the load application direction during testing.

R34 contained cuboidal γ′ precipitates (Ni_3Al/Ti) with an equivalent mean diameter of about 555 nm and a volume fraction of about 55%, as well as spherical Y_2O_3 dispersoids with a mean diameter of about 30 nm and a volume fraction around 2.1%. Both hardening particle types are practically homogeneously distributed throughout the material (Ref 14). R90 and R901315 had similar particle structures with some deviations due to different heat treatments. In addition, R901315 showed a relatively high concentration of precipitates at grain boundaries as compared to R90 due to the additional grain-coarsening heat treatment done on this batch (Ref 11). These variations in hardening particle structure between the batches induce some error in the estimated grain boundary strengthening contributions. However, this is of minor relevance for this study which focuses on investigating the overall intermediate temperature transition of the grain size effect on material strength.

Compression tests at a constant true strain rate of 10^{-4} s^{-1} are carried out on cylindrical samples with 6 mm height and 4 mm diameter between room temperature and 1200 °C using a computer-controlled electromechanical testing machine INSTRON 8562. Deformation processes within grains such as dislocation glide and creep, particle overcoming processes including climbing and interfacial pinning of dislocations (Ref 13), as well as volume diffusion are assumed to be similar in all the batches. In addition, the ⟨101⟩ fiber texture in R34 was shown not to provide any substantial change in material strength, but rather leads to a slight softening (Ref 15); therefore, its effect has been neglected in this study. Based on the above observations and assumptions, the impact of grain size on material strength is estimated as the difference between the strength of the finer grain materials (R90 and R901315) and that of the coarse and elongated reference material R34. Positive and negative differences refer to strengthening and softening effects, respectively. Phenomenological empirical equations are used to fit and rationalize the variation of this effect of grain size with temperature.

3. Results and Discussion

The experimentally measured grain size's effect Δσ on the yield strength for both isotropic materials is plotted as data points against the test temperature in Fig. 2. Referring to the figure, for both materials, the contribution of grain boundary strengthening drops exponentially up to the equicohesion temperature. Grain boundary softening sets in above the equicohesion temperature, increases up to a maximum at $T_{\text{soft-max}}$, thus further reducing the strength of the material. This softening effect then drops logarithmically thereafter till the melting point is reached, reducing and later eliminating the impact of grain size on material strength. $T_{\text{soft-max}}$ is determined to be 817 °C (1090 K) and 917 °C (1190 K) for R90 and R901315, respectively. This is about 70% of PM 3030's melting point. The drop in the softening effect at temperatures above $T_{\text{soft-max}}$ can well be rationalized by the overwhelming dominance of volume diffusion over grain boundary diffusion at temperatures close to the melting point (Ref 16).

The conventional Hall–Petch equation is used to describe test data at low temperatures:

$$\Delta\sigma_{H-P} = \alpha G_A b d^{-1/2} \quad \text{(Eq 1)}$$

where α is the grain boundary strengthening coefficient and is determined as a fit constant; b is the Burger's vector for

dislocation motion in {111}⟨110⟩ glide systems; d is the grain size, and G_A is the anisotropic shear modulus. For the purpose of this study, room temperature (RT = 22 °C) behavior is taken as reference in order to investigated the change in grain boundary strengthening with temperature. Accordingly, a value of $\alpha = \alpha_{RT} = 28$ is found to yield an overall best correlation of test results; the R90 data are slightly underestimated while the R901315 data are overestimated at low temperatures as shown in Fig. 2. Since oxide dispersion and γ' precipitation contributions are assumed identical in all the batches for estimating grain boundary strengthening, this discrepancy between the Hall–Petch model and $\Delta\sigma_{H\text{-}P}$ measurement data can be rationalized by the variations in hardening particle structure as described in Sect 2. For simplicity, the Burger's vector is considered constant over the investigated temperature range, and is taken as $b = 2.49 \times 10^{-4}$ μm which is the value for dislocation slip in nickel (Ref 16). The temperature dependence of grain boundary strengthening is reflected in Eq 1 solely by the drop in anisotropic shear modulus G_A with temperature. Due to lack of data for PM 3030, G_A values are taken from IN738 LC (Ref 17), a single crystal Ni-base superalloy with similar chemical composition and γ' precipitate structure as PM 3030 but with no oxide dispersoids, and interpolated to cover all the test temperatures. Figure 2 shows that the discrepancy between the Hall–Petch equation and measurement data increases exponentially at intermediate temperatures above 450 °C indicating a strong temperature-dependent drop of the grain boundary strengthening coefficient.

3.1 Exponential Drop of the Grain Boundary Strengthening Coefficient at Intermediate Temperatures

The very rapid drop in grain boundary strengthening observed above 450 °C can be proportionally translated into an exponential drop in grain boundary strengthening coefficient α in the Hall–Petch model as shown in Eq 2. This correlation is found to fit intermediate temperature test data very well.

$$\alpha = \alpha_{RT}\left(1 - \exp\left[k\left(1 - T_{Equi}/T\right)\right]\right) \qquad \text{(Eq 2)}$$

As room temperature is taken as a reference, α_{RT} is the grain boundary strengthening coefficient at room temperature as determined previously. k is a fit constant and is determined to be 9 for both R90 and R901315; it is obvious that the value of k is expected to vary with material and test conditions such as strain rate. T_{Equi} is the equicohesion temperature and was determined in previous publications (Ref 11, 18) to be around 700 °C for PM 3030; and T is the absolute temperature in Kelvin. The dependence of α on temperature is plotted in Fig. 3 and the resulting corrected Hall–Petch curve is shown in Fig. 2 for both isotropic fine grain materials. Because the fundamental meaning of equicohesion is that grain interior and grain boundary have identical strength, it is noteworthy that Eq 2 is written to yield α equal to zero at equicohesion temperature. It is also noteworthy that this approach describes test data even above the equicohesion point up to temperatures close to $T_{soft\text{-}max}$, the point of maximum reduction in yield strength due to fine grains. This suggests that dislocation slip remains a significant deformation mechanism, and grain boundaries still obstruct dislocation motion to a great extent at intermediate temperatures. However, rapid diffusion along grain boundaries associated with rapid recovery and annihilation of dislocations seem to counteract dislocation pile-up thereby reducing the

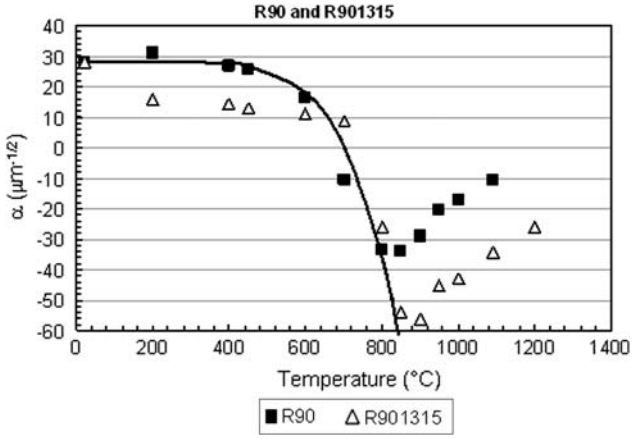

Fig. 3 Exponential temperature-dependent drop of the grain boundary strengthening coefficient used for the Hall–Petch model

advantage of finer grains in the lower intermediate temperature range. This softening effect of grain boundaries ultimately leads to even lower strength for fine grains as compared to single crystals or coarse grains above the equicohesion point. Because the density of grain boundaries increases as the grain size decreases, it can be seen in Fig. 2 that R90 shows both a higher grain boundary strengthening contribution at lower temperatures and a larger softening effect above the equicohesion temperature in agreement with previous observations (Ref 19). Therefore, it can be concluded that while very fine grains are conventionally known to provide best mechanical properties at low temperatures, intermediate grain sizes may provide better properties at intermediate temperatures, particularly above the equicohesion point.

3.2 Grain Boundary Diffusion as Rational for the Drop in Grain Boundary Strengthening and Onset of Grain Boundary Softening at Intermediate and High Temperatures

The drop in grain boundary strengthening can be rationalized by the fact that as the temperature increases diffusion becomes stronger. It should be noted that grain boundary strengthening as described by the Hall–Petch equation is based on an increase in dislocation density as a result of stronger dislocation pile-up in finer grain materials (Ref 8). Diffusion, particularly along grain boundaries, can facilitate recovery or dislocation annihilation near grain boundaries leading to a reduction in dislocation pile-up and strengthening capability of fine grains. Moreover, strong diffusion along grain boundaries promotes grain boundary deformation processes and possibly grain boundary sliding. Contrary to conventional knowledge, it was demonstrated in previous publications (Ref 20, 21) that the concept of diffusion can well be applied to deformation at relatively high strain rates such as for the compression tests used in this study. This can be rationalized by the fact that load- and temperature-supported diffusion can take place at relative high speeds consistent with rapid deformation. In fact, large uniform plastic deformation (above 80%) was observed in the isotropic fine grain batch of PM 3030 (R90) during compression testing with stress exponent values around 2. Because such a nearly superplastic flow behavior with low stress exponent can practically not result alone from dislocation mechanisms within grains, it was rationalized by primarily grain boundary

diffusion and deformation processes and possibly grain boundary sliding.

Grain boundary diffusion and deformation processes can be considered separately and then superimposed to the obstruction of dislocation motion by grain boundaries as described by the Hall–Petch equation. For this purpose, a correction factor of $c = 1.1$ and 0.6 is applied to the Hall–Petch equation (Eq 3) for R90 and R901315, respectively, to account for differences in oxide dispersoid and γ' precipitate structure in the three investigated batches; c allows to best fit test data in the low temperature range and better rationalize the intermediate temperature transition. Furthermore, a new phenomenological empirical equation is proposed that includes the grain boundary diffusion coefficient, D_b, as well as the thickness, δ, of grain boundaries. Both parameters are known to control diffusion along grain boundaries (Ref 16). In order to better understand the strength transition, the temperature dependence of diffusion processes is initially assumed to solely result from the variation in δD_b value according to the Arrhenius equation (Eq 4). Accordingly, λ in Eq 5 is considered constant, independent of temperature.

$$\Delta\sigma_{H-P} = c\alpha G_A b d^{-1/2} \quad \text{(Eq 3)}$$

$$\delta D_b = \delta D_{b0} * \exp(-Q_b/RT) \quad \text{(Eq 4)}$$

In Eq 4, Q_b is the activation energy for grain boundary diffusion, R is the universal gas constant ($R = 8.314$ J/(mol K)), and T is the temperature in Kelvin. Values for Q_b and δD_{b0} corresponding to those of nickel ($Q_b = 115$ kJ/mol and $\delta D_{b0} = 3.5.10^{-15}$ m^3/s) are used. All the diffusion constants are taken from literature (Ref 16). Volume diffusion is assumed to take place in fine and coarse grains or single crystals equally and is therefore not considered in this equation. The high temperature softening effect, $\Delta\sigma_{Diff}$, is expressed as follows:

$$\Delta\sigma_{Diff} = -\lambda\delta D_b d^{-1/3} \quad \text{(Eq 5)}$$

As evidenced by observing the thin (Hall–Petch) and bold (diffusion-based) dotted lines in Fig. 4 and 6 for R90 and R901315, respectively, considering α and λ constants results in a rather weak temperature dependence of the grain size effect on material strength. Therefore, it can be concluded that similar to the grain boundary strengthening coefficient, the fit constant λ (grain boundary softening coefficient) in Eq 5 varies strongly with temperature, material, and test conditions, which primarily explains the variation in grain boundary effect on strength. For the purpose of this study, $\lambda = 1.4 \times 10^{17}$ MPa * s is determined to best fit the maximum grain boundary softening effect corresponding to the minimum of the Δσ versus T curve at $T_{soft\text{-}max}$.

The procedure so far described in this section allows analyzing the change in grain boundary effect by considering a transition from maximum possible strengthening at room temperature as described by the corrected Hall–Petch equation to maximum possible softening at $T_{soft\text{-}max}$ as assessed by the diffusion-based equation. In this article, linear and exponential transition functions f_T are assumed. Both are defined for any temperature T in the transition range as follows:

$$\Delta\sigma_{overall} = f_T(T) = (1-s)\Delta\sigma_{H-P} + s\Delta\sigma_{Diff} \quad \text{(Eq 6)}$$

where s for the linear case is given as follows:

$$s = (T - T_S)/(T_{soft-max} - T_S) \quad \text{(Eq 7)}$$

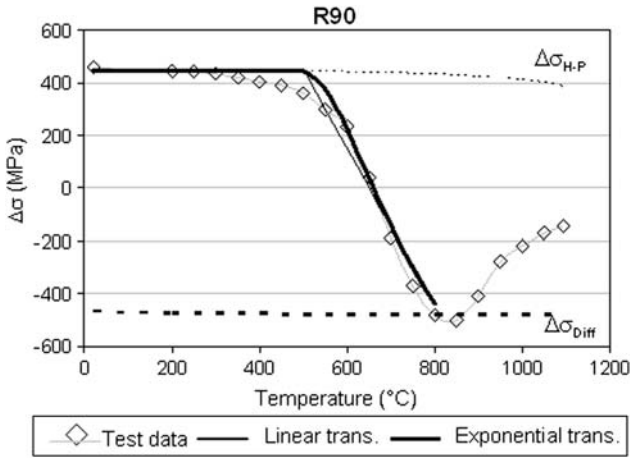

Fig. 4 Temperature dependence of the impact of grain size on the yield strength of R90: curves resulting from Hall–Petch (hatched thin line) and diffusion-based (hatched bold line) equations as well as the overall data fit using linear (thin solid line) and exponential (bold solid line) transitions at intermediate temperature are plotted. The relatively weak temperature dependence of the Hall–Petch and diffusion-based equations as seen in the graph illustrates that the strong temperature-dependent change in grain size effect can be directly correlated with a strong variation in grain boundary strengthening (α) and softening (λ) coefficients

and s for the exponential case is given as follows:

$$s = \exp[1 - (T_{soft-max} - T_S)/(T - T_S)] \quad \text{(Eq 8)}$$

$T_{soft\text{-}max}$ is considered the upper temperature limit for the transition function. T_S is the start temperature for the transition below which the overall value ($\Delta\sigma_{overall}$) for the grain boundary effect on yield strength is set equal to that calculated using the corrected conventional Hall–Petch equation without any contribution of grain boundary softening. Since there is no established analytical approach to reliably predict the interplay between the obstruction of dislocation motion by grain boundaries and the counteracting grain boundary diffusion and deformation processes, T_S is determined using numerical considerations. T_S is selected to yield best fit of the overall phenomenological equation proposed in Eq 6 to the test data by minimizing the sum square error (SSE). Within this study context, the SSE is defined as the sum of all square errors calculated at 50 °C intervals within the range from room temperature to $T_{soft\text{-}max}$. Figure 5 and 7 show the variation of the sum square error as a function of the start temperature (T_S) for both linear and exponential transition equations for R90 and R901315, respectively. For each transition function and material combination, the start temperature T_S used for the final transition equation is that at the minimum of the SSE versus T_S curves. In summary, the overall equation ($\Delta\sigma_{overall}$) is equal to: (i) the corrected conventional Hall–Petch equation below the transition temperature range assuming a constant grain boundary strengthening coefficient α as determined at the reference temperature (RT); (ii) the novel diffusion-based equation with a constant grain boundary softening coefficient as determined at $T_{soft\text{-}max}$; and (iii) the transition equation in the transition range as follows:

$$T \le T_S : \Delta\sigma_{overall} = \Delta\sigma_{H-P} \quad \text{(Eq 9)}$$

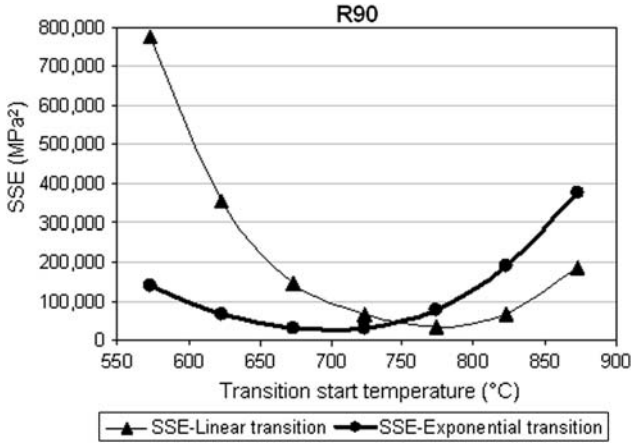

Fig. 5 Sum square error (SSE) dependence on the transition start temperature as obtained using linear (thin solid line) and exponential (bold solid line) transition functions for R90. The start temperature at minimum SSE was used for the final data fit equation

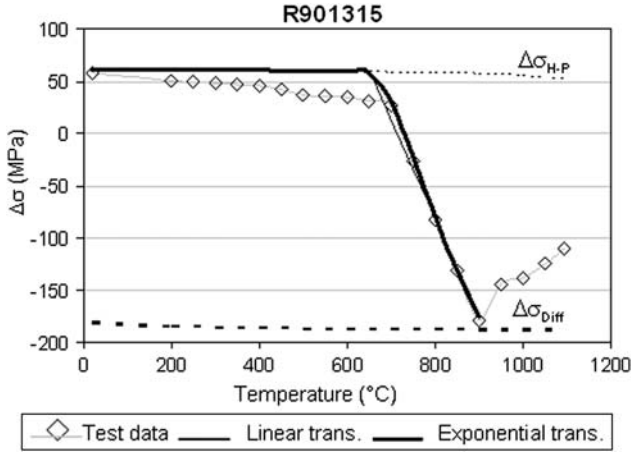

Fig. 6 Temperature dependence of the impact of grain size on the yield strength of R901315: curves resulting from Hall–Petch (hatched thin line) and diffusion-based (hatched bold line) equations as well as the overall data fit using linear (thin solid line) and exponential (bold solid line) transitions at intermediate temperature are plotted. The relatively weak temperature dependence of the Hall–Petch and diffusion-based equations as seen in the graph illustrates that the strong temperature-dependent change in grain size effect can be directly correlated with a strong variation in grain boundary strengthening (α) and softening (λ) coefficients

$$T_S \leq T \leq T_{\text{soft-max}} : \Delta\sigma_{\text{overall}} = f_T(T) \quad \text{(Eq 10)}$$

$$T = T_{\text{soft-max}} : \Delta\sigma_{\text{overall}} = \Delta\sigma_{\text{Diff}} \quad \text{(Eq 11)}$$

It should be noted that both linear and exponential transition equations yield a nearly balanced overall impact of fine grains on material yield strength at the equicohesion temperature (grain boundary strengthening contribution close to 0 MPa) for both the investigated fine grain batches. This demonstrates the excellent correlation between test data and the described empirical methodology. However, Fig. 4-7 show that the exponential transition function provides a lower SSE and a slightly better fit of test data.

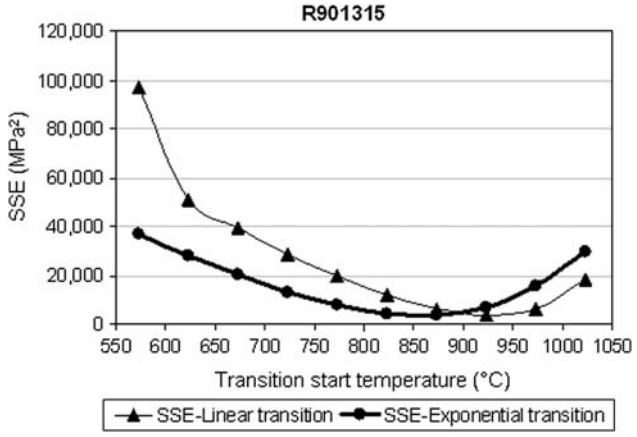

Fig. 7 Sum square error (SSE) dependence on the transition start temperature as obtained using linear (thin solid line) and exponential (bold solid line) transition functions for R901315. The start temperature at minimum SSE was used for the final data fit equation

It should be further noted that fitting data above $T_{\text{soft-max}}$ can be done by developing an equation to describe the logarithmic drop in λ. However, this is not done in this study since higher temperatures are generally not relevant for fine grain materials because of ensuing excessive diffusion resulting in too low strength to be of any technological significance. Furthermore, the volume diffusion is expected to dominate above $T_{\text{soft-max}}$ as mentioned earlier, making the material strength practically independent of grain size and grain structure as temperature increases toward melting of the material.

4. Summary and Conclusions

The intermediate temperature transition of the impact of grain size on the strength of an oxide dispersion and γ′ precipitation-strengthened nickel base superalloy PM 3030 has been investigated. Because some diffusion is already possible at temperatures far below the equicohesion point, the grain boundary strengthening contribution to material strength drops strongly with temperature corresponding to an exponential decrease in grain boundary strengthening coefficient in the Hall–Petch equation. This exponential drop applies at intermediate temperatures even above the equicohesion range up to the temperature of maximum softening at around 70% of the melting point. Alternatively, intermediate and high temperature strength drop and softening due to polycrystalline fine grain can well be rationalized by three-dimensional diffusion along grain boundaries. In the latter case, the transition from low temperature to high temperature behavior can be described by an exponential transition from the Hall–Petch strengthening behavior to grain boundary diffusion-controlled softening. Overall, the article provides a contribution in describing the critical importance of equicohesion temperature and transition in grain size effect, strengthening or softening, on material strength. It also highlights the knowledge that while fine grains even down to the nano-size are commonly desired for low temperature applications, intermediate grain sizes can be advantageous for intermediate temperature applications due to substantially limited grain boundary diffusion and deformation

processes. This can be particularly useful for key components in gas and aircraft turbines, as well as many other engine applications. Furthermore, this can be crucial for material and manufacturing process optimizations as well as well-informed approaches for material selection, dimensioning, and design for intermediate temperature applications.

References

1. E.O. Hall, The Deformation of Mild Steel: III Discussion of Results, *Phys. Soc. B*, 1951, **64**, p 747–753
2. N.J. Petch, The Cleavage Strength of Polycrystals, *J. Iron Steel Inst.*, 1953, **174**, p 25–28
3. W.A. Counts, M.V. Braginsky, C.C. Battaile, and E.A. Holm, Predicting the Hall-Petch Effect in FCC Metals Using Non-local Crystal Plasticity, *Int. J. Plast.*, 2008, **24**, p 1243–1263
4. R. Raj and M.F. Ashby, On the Grain Boundary Sliding and Diffusional Creep, *Metall. Trans.*, 1971, **2**, p 1113–1127
5. J.R. Spingarn and W.D. Nix, Diffusional Creep and Diffusionally Accommodated Grain Rearrangement, *Acta Metall.*, 1978, **26**, p 1389–1398
6. I.S. Servi and N.J. Grant, Creep and Stress Rupture Behavior of Aluminum as a Function of Purity, *J. Metals,* 1951, p 909–916
7. I.S. Servi and N.J. Grant, Structure Observations of Aluminum Deformed in Creep at Elevated Temperature, *J. Metals,* 1951, p 917–922
8. G.E. Dieter, *Mechanical Metallurgy*, SI Metric Editions, McGraw-Hill Book Company, London, 1986
9. R.L. Cairns, L.R. Curwick, and J.S. Benjamin, Grain Growth in Dispersion Strengthened Superalloys by Moving Zone Heat Treatments, *Metall. Trans. A*, 1975, **6**, p 179–188
10. J.S. Benjamin, Dispersion Strengthened Superalloys by Mechanical Alloying, *Metall. Trans.*, 1970, **1**, p 2943–2951
11. M. Nganbe and M. Heilmaier, High Temperature Strength and Failure of the Ni-base Superalloy PM 3030, *Int. J. Plast.*, 2009, **25**, p 822–837
12. B. deMestral, G. Eggeler, and H.-J. Klam, On the Influence of Grain Morphology on the Creep Deformation and Damage Mechanisms in Directionally Solidified and Oxide Dispersion Strengthened Superalloys, *Metall. Mater. Trans. A*, 1996, **27**, p 879–890
13. J.J. Stevens and W.D. Nix, The Effect of Grain Morphology on Longitudinal Creep Properties of INCONEL MA 754 at Elevated Temperature, *Metall. Mater. Trans. A*, 1985, **16**, p 1307–1324
14. M. Nganbe and M. Heilmaier, Modelling of Particle Strengthening in the γ' and Oxide Dispersion Strengthened Nickel-base Superalloy PM 3030, *Mater. Sci. Eng. A*, 2004, **387–389**, p 609–612
15. R.F. Singer, R.C. Benn, and S.K. Kang, Creep Rupture Properties of Inconel Alloy MA 6000, *Frontiers of High Temperature Materials*, J.S. Benjamin and R.C. Benn, Ed., Inco Alloy Product Company, 1983, Vol. 2, p 336–357
16. H.J. Frost and M.F. Ashby, *Deformation-Mechanism-Maps. The Plasticity and Creep of Metals and Ceramics*, Pergamon Press, Oxford, 1982
17. U. Bayerlein, Zur Ermittlung der Textur- und Gefügeabhängigkeit der Elastischen Eigenschaften Sowie der Einkristallkonstanten von Superlegierungen bei Höheren Temperaturen (on the Determination of the Texture and Grain Structure Dependence of the Elastic Properties and Single Crystal Constants of Superalloys at High Temperatures), *VDI Fortschrifttsberichte*, 1991, **5**(236), Düsseldorf (in German)
18. M. Nganbe, M. Heilmaier, and L. Schultz, Dependence of Mechanical Strength on Grain Structure in the γ' and Oxide Dispersion Strengthened Nickelbase Superalloy PM 3030, *Z. Metallkunde*, 2005, **96**(6), p 625–631
19. M. Mabuchi and K. Higashi, Strengthening Mechanisms of Mg-Si Alloys, *Acta Mater.*, 1996, **44**(11), p 4611–4618
20. M. Nganbe, "Untersuchung und Optimierung der γ'- und Oxid-dispersionsgehärteten (ODS) Nickelbasissuperlegierung PM 3030 (Investigation and Optimization of the γ'- and Oxide Dispersion Strengthened (ODS) Nickel-base Superalloy PM 3030," Dissertation thesis, Cuviller Verlag, Göttingen, 2002 (in German)
21. M. Heilmaier, M. Nganbe, and F.E.H. Müller, On the Creep and Superplastic Behavior of the ODS Nickel-based Superalloy PM 3030, Honorary Symposium for Professor Oleg D. Sherby, *Deformation, Processing and Properties of Structural Materials*, E.M. Taleff et al., Ed. (Warrendale, PA), TMS, 2000, p 287–298